71.013(2)°, $\gamma = 72.862(2)°$, $V = 1260.7(5)$ Å^3, $\rho_{calc} = 1.255$ g cm^{-3}, $\mu = 0.82$ cm^{-1} (no correction), $Z = 1$, $Mo_{K\alpha}$ radiation, 7007 unique reflections($R_{int} = 0.043$), $2\theta_{max} = 60°$ (4661 observed, $I > 3\sigma(I)$, $R = 0.063$, $Rw = 0.067$). Crystallographic data (excluding structure factors) for the structures reported in this paper have been deposited with the Cambridge Crystallographic Data Centre as supplementary publication no. CCDC-136348 and -136349. Copies of the data can be obtained free of charge on application to CCDC, 12 Union Road, Cambridge CB2 1EZ, UK (fax: (+44) 1223-336-033; e-mail: deposit@ccdc.cam.ac.uk).

[9] Synthesis of $(CS_2) \subset [\{Ni(tmtaa)\}_2]_6$. A CS_2 solution of [Ni(tmtaa)] (50 mg, 20 mL) was mixed with a CS_2 solution of anthracene (18 mg, 20 mL). The mixure was layered with hexane (equal volume) and allowed to evaporate slowly (m.p. 241–245 °C). Elemental analysis [%]: calcd: C 65.09, H 5.44, N 13.75; found: C 64.98, H 5.47, N 13.68. Crystal structure analysis: Enraf-Nonius Kappa CCD diffractometer, $T = 123$ K, crystal mounted in oil. $Ni_{12}C_{265}H_{264}N_{48}S_2$, $M = 4889.84$, $R\bar{3}(h)$ (No. 148), $a = 41.5300(17)$, $c = 11.6099(17)$ Å, $V = 17\,341.3(0.8)$ Å^3.

[10] V. L. Goedken, M. C. Weiss, *Inorganic Syntheses* **1980**, *XX*, 115.

Globular Amphiphiles: Membrane-Forming Hexaadducts of C_{60}**

Michael Brettreich, Stephan Burghardt, Christoph Böttcher, Thomas Bayerl, Sybille Bayerl, and Andreas Hirsch*

Most of the biological membrane-forming lipids are double-chain phospho- or glycolipids with 16–22 carbon atoms per chain and which may be mono- or polyunsaturated. They perform many functions in biological systems. At the interface between biology and materials sciences, the development of artifical nanostructures as mimics of natural systems or as prototypes of novel functional aggregates is playing an important role. This article describes the synthesis and the membrane and vesicle formation of a new class of artificial lipids. They have a globular structure with the spherical C_{60} being used to define the molecular geometry. Five pairs of dodecyl chains and one pair of polyamide dendrons are bound to C_{60} in an octahedral [1:5]-addition pattern[1] by methylene bridges.[2]

For a synthesis of the globular amphiphile **1** (see Scheme 2), the alcohol[3] **2** and malonyl dichloride were allowed to react to yield malonate **3**. A nucleophilic cyclopropanation reaction[4, 5] of C_{60} with **3** leads to the monoadduct **4** (Scheme 1).

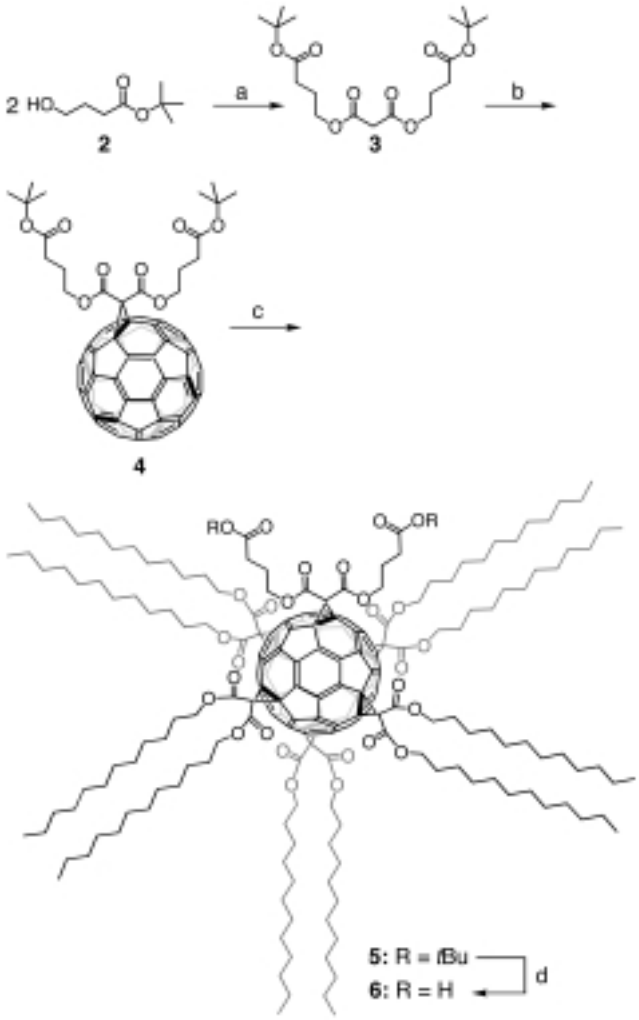

Scheme 1. Syntheses of dicarboxylic acid **6**. a) Malonyldichloride, pyridine, CH_2Cl_2; b) C_{60}, DBU, CBr_4, toluene; c) 1) DMA, 2) CBr_4, DBU, didodecyl malonate, toluene; d) TFA, toluene. DBU = 1,8-diazabicyclo[5.4.0]undec-7-ene, DMA = dimethylanthracene, TFA = trifluoroacetic acid.

The five pairs of lipophilic C_{12} chains, which are in octahedral positions relative to the first addend (Figure 1), were inserted in one step by cyclopropanation of **4** with didodecyl malonate,

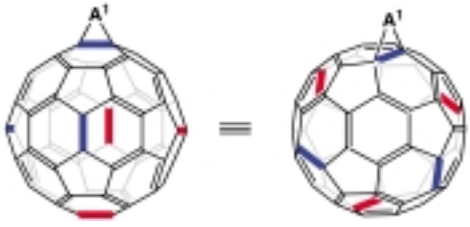

Figure 1. Octahedral positions relative to the first addend A^1 in a C_{2v} symmetrical hexaadduct of C_{60}.

[*] Prof. Dr. A. Hirsch, Dipl.-Chem. M. Brettreich, S. Burghardt
Institut für Organische Chemie
Universität Erlangen-Nürnberg
Henkestrasse 42, 91054 Erlangen (Germany)
Fax: (+49) 9131-852-6864
E-mail: hirsch@organik.uni-erlangen.de

Dr. C. Böttcher
Forschungszentrum für Elektronenmikroskopie
Institut für Chemie, Freie Universität Berlin
14195 Berlin (Germany)

Prof. Dr. T. Bayerl, Dr. S. Bayerl
Physikalisches Institut EP-5,
Universität Würzburg, 97074 Würzburg (Germany)

[**] This work was been supported by the Deutsche Forschungsgemeinschaft and by the Fonds der Chemischen Industrie. We thank Dr. K. Fischer and Prof. Dr. K. Schmidt from the Institute of Physical Chemistry at the University of Mainz for performing the light scattering measurements.

Supporting information for this article is available on the WWW under http://www.wiley-vch.de/home/angewandte/ or from the author.

  0570-0833/00/3910-1845 $ 17.50+.50/0

using reversible template activation with dimethyl anthracene (DMA).[6–8] Chromatographic purification yielded 23 % of the mixed hexaadduct **5** as a viscous liquid. Compound **5** was deprotected with trifluoroacetic acid (TFA), and **6** was isolated in a 93 % yield as a yellow waxlike solid (Scheme 1). Amide dendron **7**,[9] which was generated convergently, was

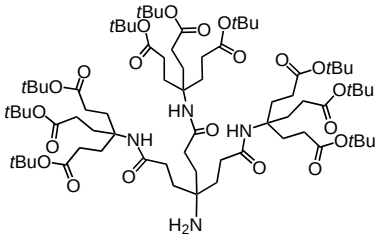

7

added using *N*,*N*′-dicyclohexylcarbodiimide and 1-hydroxybenzotriazol to give dendrimer **8** in a 30 % yield. The *tert*-butyl groups were removed by TFA and the target molecule **1** was obtained as a yellow powder in 96 % yield, with a melting point of 186 °C (Scheme 2).

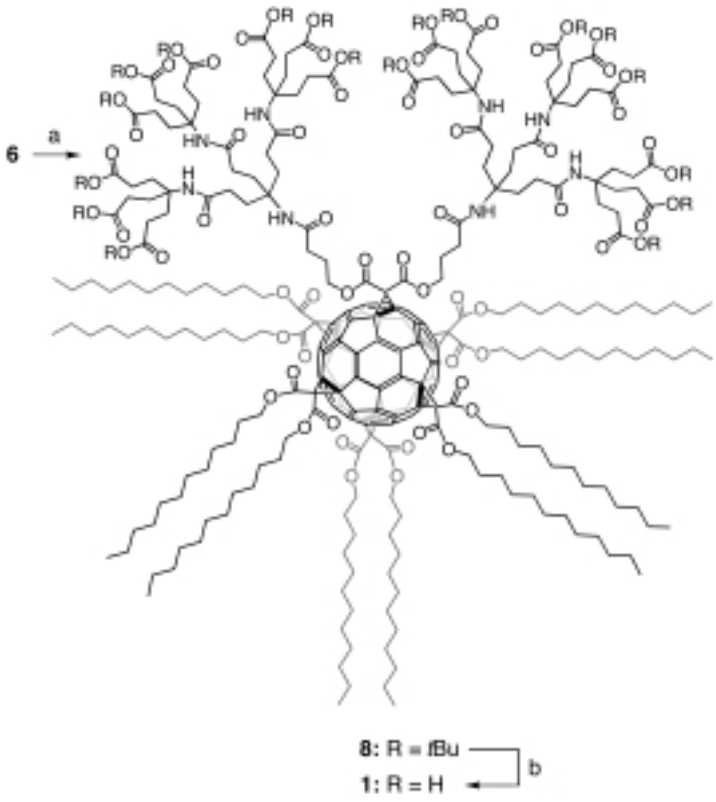

Scheme 2. Syntheses of the globular amphiphile **1**. a) **7**, DCC, HOBt, THF; b) TFA, toluene. HOBt = 1-hydroxy-1*H*-benzotriazole.

Compounds **1**, **3**–**6**, and **8** were fully characterized by ^{1}H NMR, ^{13}C NMR, IR, and UV/Vis spectroscopy, as well as by mass spectrometry.[10] The spectroscopic properties are characteristic for C_{2v} symmetrical monoaddition compounds[11] or C_{2v} symmetrical hexaaddition compounds with an octahedral [1:5]-addition pattern.[6]

In order to visualize the structure of the globular amphiphile **1**, we first performed molecular dynamics simulations.[12] Figure 2 shows the result of this computation. The two types

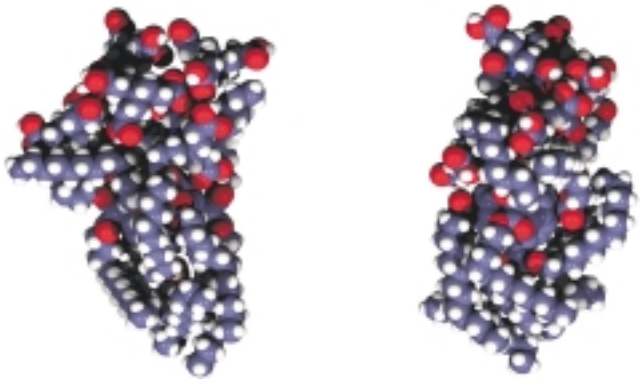

Figure 2. Molecular dynamics simulation of **1** (orthogonal views). Conditions: Heating time 5 ps, run time 15 ps, cooling time 50 ps, step size 0.001 ps, starting temperature 0 K, simulation temperature 1000 K, final temperature 0 K, in vacuum.

of addends are located in two areas which are, to a large extent, separated from each other. The densely packed hydrophilic and hydrophobic regions almost completely enclose the C_{60} core. The average dimension of about 3.5 nm along the main polar axis is similar to that of natural phospho- or glycolipids. In contrast, the typical diameters of 1.4–2.3 nm found in directions perpendicular to this axis are considerably larger than those found for natural double-chain lipids (diameters of about 0.7 nm).

At pH 7.4 (phosphate buffer) the globular amphiphile **1** slowly disperses in water to form streaks. Large flakes appear until, after several minutes, a stable, yellow opalescent solution develops. This kind of opalescence is typical for colloidal solutions with particle sizes below the wavelength of light, that is, below 400 nm. Higher concentrations (>3 mg mL^{-1}) will, after several hours, precipitate a highly viscous and intensively light-scattering phase from the clear solution above.

Aggregation behavior of **1** was investigated by freeze-fracture and cryo-electron microscopy. Freeze-fracture electron microscopy of the yellow opalescent solution described above reveals distinctly vesicular structures. The diameters of the vesicles range from 100 to 400 nm and can, therefore, be the cause of the opalescence (Figure 3). Not a single freeze fracture shows multilamellar structures, which indicates a preference for the formation of single-layer (unilamellar) vesicles. The vesicle dimensions found are similar to those of natural lipids (such as lecithine). The propensity to form unilamellar structures seems to be assisted by the high density of negative charges (at pH 7.4) in the hydrophilic part of **1**. Cryo-electron microscopy (cryo-TEM) also reveals the vesicular structures, with this method providing an even more precise picture. It allows thin layers (100 to 200 nm) of the amorphously vitrified aqueous sample to be directly imaged and gives high-resolution projection images of the uncontrasted sample in the native environment of the solvent.[13]

  0570-0833/00/3910-1846 $ 17.50+.50/0

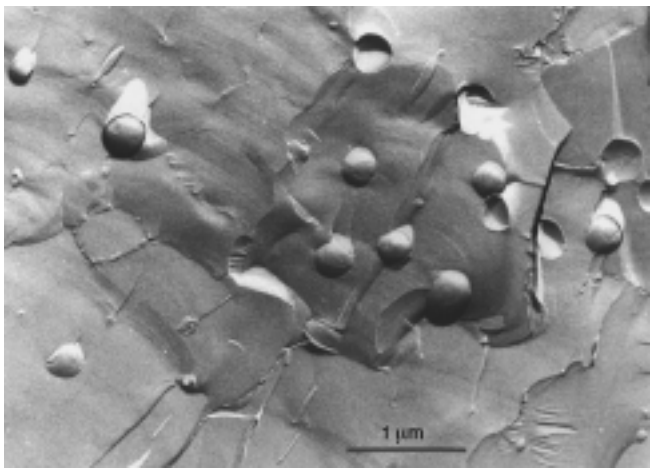

Figure 3. Freeze-fracture electron micrograph of **1** (the scale shown is 1 µm). Conditions: Solution of **1** (2 mg mL^{-1}) in phosphate buffer (pH 7.4), freezing from room temperature in liquid N_2, further details are analogous to Ref. [6e].

The cryo-TEM investigations of **1** reveal a wide variety of aggregates, the fine structure of which, however, is invariably based upon the same structural principle—the formation of double-layer membranes. The dominant structures are vesicles of dimensions ranging between 50 and 400 nm (Figure 4). Figure 4a shows the typical projection image of a spherical vesicle with a diameter of 80 nm. The density profile of the membrane is clearly resolved and the overall thickness can be determined as about 7 nm. Since the dimensions of large vesicles (>200 nm) exceed the thickness of the water lamella embedding them, such vesicles are no longer of a spherical form but show deformations (Figure 4b). Figure 4b also shows that partial formation of multilayers is possible as well.

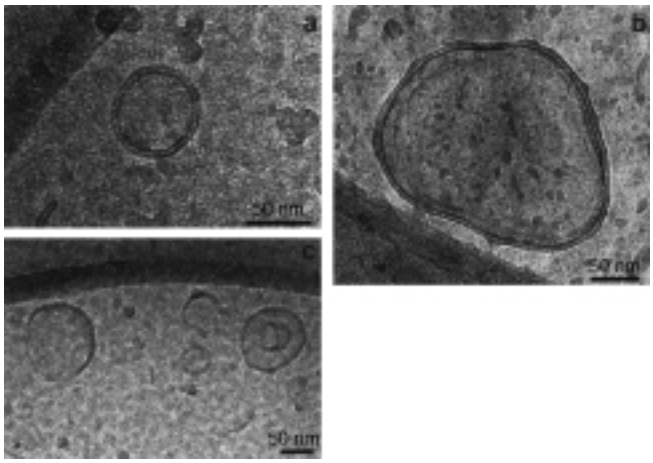

Figure 4. a) Cryo-TEM image of a vesicle of **1** (diameter 80 nm, the scale shown is 50 nm). The bilayer structure (approximate diameter 7 nm) of the membrane is clearly resolved, and the outer dark (electron-dense) regions, with a thickness of approximately 2 nm, conform well to the dimension of the hydrophilic head (compare with the model in Figure 2). The brighter inner seam with a width of approximately 3 nm is, therefore, considered to be the hydrophobic alkyl chain.[14] b) Cryo-TEM image of a deformed vesicle of **1** (diameter 400 nm, the scale shown is 50 nm). Several regions point to a multilayered growth of the membrane. c) Short membrane fragments and incomplete vesicle structures show early stages of the growth process of the membrane structures (compare with Figure 5, the scale shown is 50 nm).

In addition to vesicles, smaller cylindrical aggregates of about 5 to 200 nm in length can often be found (Figure 5). In the lateral direction, however, they are regularly of the dimension of the double-layer membrane and show the resolution of the double-layer membrane profile. As the membrane motif remains the same through a large number of investigated structures (>100), that is, they invariably show the double-layer profile, and since the aggregates have complete freedom to orient themselves in the solution, the cross-section of the cylinders may be considered circular.

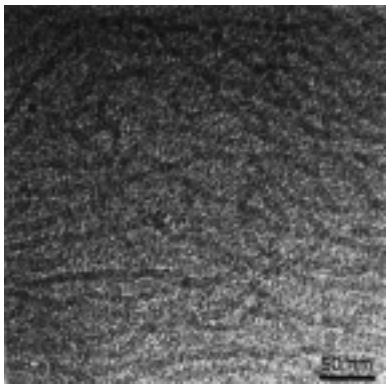

Figure 5. Cryo-TEM image of a population of cylindrical aggregates (the scale is 50 nm). The diameter (7 nm) of all aggregates, which may take on different orientations in solution, is equal and shows the resolved bilayer motif.

As a result of the high natural contrast of the electron-rich C_{60} molecules, the method also allows the smallest molecular units to be detected (Figure 6); they are spherical particles with a diameter of about 3.5 nm and, because of their dimensions, have to be considered as nonaggregated single molecules.

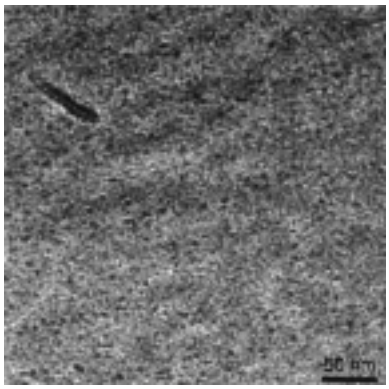

Figure 6. Cryo-TEM image of a population of spherical particles with a diameter of approximately 3.5 nm, which corresponds to the molecular dimension (the scale is 50 nm).

Light scattering tests are presently being performed, in order to investigate in more detail how the formation of aggregates is dependent upon concentration and pH value. First results show that the critical micelle concentration is very low. Aggregates of the size described above have been found up to concentrations of 3 mg l^{-1}. The amphiphile **1** has

  0570-0833/00/3910-1847 $ 17.50+.50/0

properties, such as size and vesicle-formation concentration, which are very similar to common double-chain lipids; however, they show a propensity to form unilamellar aggregates, as well as a variety of different bilayered structures.

Received: December 27, 1999 [Z14469]

[1] A. Hirsch, I. Lamparth, T. Grösser, H. R. Karfunkel, *J. Am. Chem. Soc.* **1994**, *116*, 9385 – 9386.

[2] For self-assembly of ionic monoadducts of C_{60} and the behavior of these compounds at the air/water interface, see: a) A. M. Cassell, C. L. Asplund, J. M. Tour, *Angew. Chem.* **1999**, *111*, 2565 – 2568; *Angew. Chem. Int. Ed.* **1999**, *38*, 2403 – 2405; b) H. Murakami, M. Shirakusa, T. Sagara, N. Nakashima, *Chem. Lett.* **1999**, 815 – 816; c) F. Cardullo, F. Diederich, L. Echegoyen, T. Habicher, N. Jayaraman, R. M. Leblanc, J. F. Stoddart, S. Wang, *Langmuir* **1998**, *14*, 1955 – 1959; d) U. Jonas, F. Cardullo, P. Belik, F. Diederich, A. Gügel, E. Harth, A. Herrmann, L. Isaacs, K. Müllen, H. Ringsdorf, C. Thilgen, P. Uhlmann, A. Vasella, C. A. A. Waldraff, M. Walter, *Chem. Eur. J.* **1995**, *1*, 243 – 251.

[3] H. R. Kricheldorf, J. Kaschig, *Liebigs Ann. Chem.* **1976**, 882 – 890.

[4] X. Camps, A. Hirsch, *J. Chem. Soc. Perkin Trans. 1* **1997**, 1595 – 1596.

[5] C. Bingel, *Chem. Ber.* **1993**, *126*, 1957 – 1959.

[6] a) I. Lamparth, C. Maichle-Mössmer, A. Hirsch, *Angew. Chem.* **1995**, *107*, 1755 – 1757; *Angew. Chem. Int. Ed.* **1995**, *34*, 1607; b) I. Lamparth, A. Herzog, A. Hirsch, *Tetrahedron* **1996**, *52*, 5065 – 5075; c) X. Camps, H. Schönberger, A. Hirsch, *Chem. Eur. J.* **1997**, *3*, 561 – 567; d) X. Camps, E. Dietel, A. Hirsch, S. Pyo, L. Echegoyen, S. Hackbarth, B. Roeder, *Chem. Eur. J.* **1999**, *5*, 2362 – 2373; e) M. Hetzer, S. Bayerl, X. Camps, O. Vostrowsky, A. Hirsch, T. M. Bayerl, *Adv. Mater.* **1997**, *9*, 913 – 917; f) M. Hetzer, H. Clausen-Schaumann, S. Bayerl, T. M. Bayerl, X. Camps, O. Vostrowsky, A. Hirsch, *Angew. Chem.* **1999**, *11*, 2103 – 2106; *Angew. Chem. Int. Ed.* **1999**, *38*, 1962 – 1965; g) A. Herzog, O. Vostrowsky, A. Hirsch, *Eur. J. Org. Chem.* **2000**, 171 – 180; h) F. Djojo, E. Ravanelli, O. Vostrowsky, A. Hirsch, *Eur. J. Org. Chem.* **2000**, 1051 – 1059.

[7] A. Hirsch, *Top. Curr. Chem.* **1999**, *199*, 1.

[8] F. Diederich, D. Kessinger, *Acc. Chem. Res.* **1999**, *32*, 537 – 545.

[9] a) M. Brettreich, A. Hirsch, *Tetrahedron Lett.* **1998**, *39*, 2731 – 2734; b) M. Brettreich, A. Hirsch, *Synlett* **1998**, 1396 – 1398.

[10] Complete experimental data of compounds **1**, **4** – **6**, and **8** are available in the "supporting information". Data for **3** can be obtained from the author.

[11] A. Hirsch in *The Chemistry of the Fullerenes*, Thieme Organic Chemistry Monograph Series, Stuttgart, **1994**.

[12] HyperChem, Release 5, Hypercube Inc., Ontario, Canada, **1996**.

[13] M. Adrian, J. Dubochet, J. Lepault, A. W. Dowall, *Nature* **1984**, *308*, 32.

[14] C. Böttcher, H. Stark, M. van Heel, *Ultramicroscopy* **1996**, *62*, 133.

In Situ Monitoring of a Heterogeneous Palladium-Based Polyketone Catalyst**

Wilhelmus P. Mul,* Heiko Oosterbeek, Gerhard A. Beitel, Gert-Jan Kramer, and Eite Drent

In the early 1980s a class of very active palladium catalysts was discovered which allowed the synthesis of a perfectly alternating aliphatic polyketone ($n\,CH_2CH_2 + n\,CO \rightarrow [CH_2CH_2C(O)]_n$) in an efficient way.[1–3] These catalysts consist of a Pd^{II} center, a bidentate chelating ligand, and two weakly associated anions. The origin of the perfectly alternating nature of the copolymers has received ample attention, both in experimental[1, 3–7] and in theoretical studies.[8–10] The mechanism for copolymer chain growth involves two sequential propagation steps: migratory CO insertion into the Pd – alkyl bond of the growing polymer chain followed by migratory ethene insertion into the resulting Pd – acyl bond. There is consensus that double CO insertion does not occur for thermodynamic reasons, while double ethene insertion is kinetically hampered due to the higher affinity of Pd^{II} centers for CO over ethene. However, thus far all experimental mechanistic studies focused on copolymerization in solution, while under actual process conditions (slurry or gas-phase), the initially single-site Pd catalyst is heterogenized and resides on the surface or in the bulk of the copolymer.

While there are several analytical techniques for the in situ study of single-site catalysts in the liquid state,[11, 12] there is a lack of techniques to directly monitor catalysis at supported single-site catalysts.[13] Polarization modulation reflection absorption infrared spectroscopy (PM-RAIRS) is an adaptation of the well-known RAIRS technique for studying species adsorbed at metal surfaces with submonolayer sensitivity, allowing the detection of signals normally obscured by huge gas-phase absorptions.[14–16] We used PM-RAIRS to monitor CO/ethene copolymerization at the single-site Pd catalyst [(dppp)Pd(CH_3)(OTf)] (**1**; dppp = 1,3-bis(diphenylphosphanyl)propane; OTf = OSO_2CF_3 = triflate) in the microcrystalline state (in the absence of any solvent), and focused on two aspects of the process: single insertion steps and copolymer growth.

Single insertion steps could be observed by alternately exposing the catalyst to CO and ethene atmospheres. Starting from **1**, sequential addition and removal of CO, ethene, and CO led to the stepwise formation of the six-membered

[*] Dr. W. P. Mul, H. Oosterbeek, Dr. G. A. Beitel,[+]
Prof. Dr. G.-J. Kramer, Prof. Dr. E. Drent
Shell Research and Technology Centre, Amsterdam
P.O. Box 38000, 1030 BN Amsterdam (The Netherlands)
Fax: (+31) 20-630-2930
E-mail: pim.w.p.mul@opc.shell.com

[+] Current address:
Ferroelectric Technologies, Memory products
Infineon Technologies AG, MPETF
Otto-Hahn-Ring 6, 81730 Munich (Germany)

[**] We thank Dr. H. P. C. E. Kuipers for his stimulating interest, the members of the Carilon Polymer Team within Shell for valuable discussions, and Shell International Chemicals B.V. for giving permission to publish this paper.

  0570-0833/00/3910-1848 $ 17.50+.50/0